ON THE FINITE ELEMENT ANALYSIS OF THIN-WALLED STRUCTURES WITH APPLICATION TO STRUCTURAL PROBLEMS IN REACTOR TECHNOLOGY

T. KAWAI

Institute of Industrial Science, University of Tokyo,
22-1, Roppongi 7 Chome, Minato-ku, Tokyo 106, Japan

T. MURAKI

Department of Ocean Engineering,
Massachusetts Institute of Technology, Cambridge, Massachusetts 02139, U.S.A.

T. TOYOSHI

Nuclear Power Design Office, Kawasaki Factory, Fuji Electric Co., Ltd.,
1-1, Tanabe Shinden, Kawasaki, Tokyo 210, Japan

SUMMARY

It is the authors' opinion that there must be quite a few structures which can be idealized as thin-walled beams among various structural components of the nuclear reactors and plant systems, and by developing the mass as well as stiffness matrices of such a beam element, practical finite element analysis of a thin-walled structure with variable cross section can be easily made to compare with the conventional method of analysis, the details of which can be seen in the authors' paper presented at the 3rd AF Conference on the Matrix Method of Structural Mechanics held at Dayton Ohio, October 1971, and a paper to be published in the *International Journal of Computers and Structures*, the Pergamon Press, this year.

As for numerical examples vibration and response analysis of a fuel charging machine of a nuclear reactor will be given.

The main features of the present method can be summarized as follows:

(1) A new stiffness matrix of a beam element for warping-torsion is derived by using the 3rd order polynomial.

(2) 3D stiffness matrix of a beam element whose nodal points may be arbitrarily taken on each end section can be derived by following standard matrix transformation procedure, transformation matrix of which is derived from the basic displacement function assumed in the modern theory of a thin-walled beam. Other important matrices of a beam element such as mass, intial stress and so on can be derived in the similar way.

(3) A method of calculation on the stiffness increase of a beam element due to various stiffening members or stiffness reduction due to cut-outs is proposed.

(4) Effects of deformation of a beam cross section as well as shear deformation on the beam deflection will be successfully made by a finite element method based on the extended St. Venant's semi-inverse method.

1. INTRODUCTION

In the field of structural engineering, it is a common practice to idealize slender plate structures as thin-walled beams with rigid cross sections and make stress analysis by using the modern engineering theory of beams. Ships, bridges, aircrafts, railroad trucks, large machine etc. are typical examples of such structures.
Design philosophy of these structures has been based on the bending-torsion theory of thin-walled beams proposed by many outstanding scholars such as S. P. Timoshenko, F. Bleich, V. Z. Vlasov and others before advent of electronic digital computers. With the progress of high speed digital computers the existing simply method of structural analysis based on the modern beam theory has been replaced by the finite element method of three dimensional plate structures which are more realistic idealization of actual structures. Generally, however, use of such computer programs are very expensive and time-consuming, therefore frequent use of these computing system may not be economically feasible even at large industrial firms.
It is a purpose of the present paper to propose a simplified and yet practical overall finite element analysis of a thin-walled structure based on the modern engineering theory of beams. The analysis consists of three steps, the first of which is evaluation of various section properties of a given beam structure, especially the torsional stiffness.
The second step of analysis is soultion as well as formulation of overall stiffness equation of the structure. In the formulation of overall stiffness equation, a special consideration is made on the discontinuity of nodal points which may exist between two adjacent beam elements due to variable beam cross section. The third step of this method is shear deformation analysis in which the finite element formulation of Semi-Inverse Method is proposed.

2. THEORETICAL BASIS FOR FINITE ELEMENT ANALYSIS OF THIN-WALLED STRUCTURES WITH A VARIABLE CROSS SECTION

In overall analysis of slender thin-walled structures, they are usually idealized into thin-walled beams with variable cross section. In this section, therefore, theoretical basis for finite element analysis of a thin-walled beam will be briefly described.

2.1 Recapitulation of Modern Engineering Theory of a Beam

Modern engineering theory of a beam is based on the following assumed displacement functions:

$$\left.\begin{aligned} U(x,y,z) &= u(z) - y\,\theta(z) \\ V(x,y,z) &= v(z) + x\,\theta(z) \\ W(x,y,z) &= w(z) - x\,u'(z) - y\,v'(z) + \theta'(z)\,\omega_n(x,y) \end{aligned}\right\} \quad (1)$$

where (U , V , W) represents the displacement vector of a general point, while ($u(z)$, $v(z)$) is the lateral displacement vector of the centroid, $w(z)$ is the average axial displacement of the given section and $\theta(z)$ is the angle of rotation as shown in Fig. 1. $\omega_n(x , y)$ is the so-called normalized warping function of St. Venant's torsion problem and it is defined as follows:

$$\left.\begin{aligned} \omega_n(x,y) &= \omega(x,y) - \frac{S_\omega}{A} \\ S_\omega &= \iint \omega(x,y)\,dx\,dy \\ A &= \iint dx\,dy \end{aligned}\right\} \quad (2)$$

According to the well-known St. Venant's torsion theory, $\omega(x, y)$ is defined as a solution of the following boundary value problem:

$$\Delta\omega(x, y) = 0 \tag{3}$$

with the following boundary condition:

$$\frac{\partial\omega}{\partial n} = y\cos(n, x) - x\cos(n, y) \tag{4}$$

on the boundary curve C for a simply connected region. (See Fig. 2)
It is easily shown that the corresponding variational problem of St. Venant's torsion problem is given as follows:

$$\delta\iint\frac{1}{2}G\alpha^2\left\{\left(\frac{\partial\omega}{\partial x} - y\right)^2 + \left(\frac{\partial\omega}{\partial y} + x\right)^2\right\}dx\,dy - M_z\,\delta\alpha = 0 \tag{5}$$

in which variation should be taken with respect to the warping function $\omega(x, y)$ as well as the rate of twist α .
Once the warping function $\omega(x, y)$ is determined, various section properties of warping-torsion can be calculated by the following formulae.

(i) St. Venant's torsional constant K

$$K = \iint\left\{\left(\frac{\partial\omega}{\partial x} - y\right)^2 + \left(\frac{\partial\omega}{\partial y} + x\right)^2\right\}dx\,dy \tag{6}$$

(ii) Warping torsional rigidity EI_ω with respect to the centroid

$$I_\omega = \iint\left\{\omega_n(x, y)\right\}^2 dx\,dy \tag{7}$$

(iii) Warping cross products of inertia $I_{\omega x}$, $I_{\omega y}$ with respect to the centroid

$$\left.\begin{aligned} I_{\omega x} &= \iint x\,\omega_n(x, y)\,dx\,dy \\ I_{\omega y} &= \iint y\,\omega_n(x, y)\,dx\,dy \end{aligned}\right\} \tag{8}$$

(iv) Location of shear center (x_s , y_s)

$$x_s = -\frac{I_{\omega y}}{I_{yy}} \quad , \quad y_s = \frac{I_{\omega x}}{I_{xx}} \tag{9}$$

where

$$I_{xx} = \iint x^2 dx\,dy \quad , \quad I_{yy} = \iint y^2 dx\,dy \tag{10}$$

Computer program for evaluation of these section properties is described by the author's paper presented at Wright-Patterson Air Force Base, Dayton, Ohio last October [1],[2],[3]. It is interesting to note that the so-called shear flow analysis of a thin-walled cross section is the most simplified case of analysis in this program.

2.2 Derivation of a New Stiffness Matrix of Beam Element for Warping Torsion

According to the modern theory of a beam, warping torsion of a beam is governed by the following variational equation:

$$\delta\int_0^\ell\left(\frac{1}{2}EI_\omega^{(s)}\theta''^2 + \frac{1}{2}GK\theta'^2\right)dz - \int_0^\ell m_z\,\delta\theta\,dz = 0 \tag{11}$$

where, $EI_\omega^{(s)}$ is the warping torsional rigidity of a given beam with respect to the shear center. The present autor derived the following new stiffness matrix of a beam element for warping-torsion by using the 3rd order polynomial as used in the derivation of a beam stiffness matrix for bending [4].

$$\begin{Bmatrix} M_{zL} \\ M_{zR} \\ T_L \\ T_R \end{Bmatrix} = \begin{bmatrix} \frac{12EI_\omega^{(s)}}{\ell^3}+\frac{6GK}{5\ell} & -\frac{12EI_\omega^{(s)}}{\ell^3}-\frac{6GK}{5\ell} & \frac{6EI_\omega^{(s)}}{\ell^2}+\frac{GK}{10} & \frac{6EI_\omega^{(s)}}{\ell^2}+\frac{GK}{10} \\ -\frac{12EI_\omega^{(s)}}{\ell^3}-\frac{6GK}{5\ell} & \frac{12EI_\omega^{(s)}}{\ell^3}+\frac{6GK}{5\ell} & -\frac{6EI_\omega^{(s)}}{\ell^2}-\frac{GK}{10} & -\frac{6EI_\omega^{(s)}}{\ell^2}-\frac{GK}{10} \\ \frac{6EI_\omega^{(s)}}{\ell^2}+\frac{GK}{10} & -\frac{6EI_\omega^{(s)}}{\ell^2}-\frac{GK}{10} & \frac{4EI_\omega^{(s)}}{\ell}-\frac{2GK\ell}{15} & \frac{2EI_\omega^{(s)}}{\ell}-\frac{GK\ell}{30} \\ \frac{6EI_\omega^{(s)}}{\ell^2}+\frac{GK}{10} & -\frac{6EI_\omega^{(s)}}{\ell^2}-\frac{GK}{10} & \frac{2EI_\omega^{(s)}}{\ell}-\frac{GK\ell}{30} & \frac{4EI_\omega^{(s)}}{\ell}-\frac{2GK\ell}{15} \end{bmatrix} \begin{Bmatrix} \theta_L \\ \theta_R \\ \theta'_L \\ \theta'_R \end{Bmatrix} \tag{12}$$

where (M_{zL} , M_{zR}) are the torsional moment, while (T_L , T_R) are the so-called bimoment of given beam element at both ends.

2.3 General Stiffness Matrix of a Straight Beam Element with a Constant Cross Section Which is Defined with Respect to Arbitrary Points P and Q on each end Section

With these preliminaries, the stiffness matrix of a beam element can be formulated by simply assembling bending stiffness matrices with respect to principal axes passing through the centroid [$\mathbf{K}_u$], [$\mathbf{K}_v$], the warping torsional stiffness [$\mathbf{K}_\theta$] and the stiffness matrix of axial deformation [$\mathbf{K}_w$] as follows:

$$\begin{Bmatrix} \mathbf{f}_u \\ \mathbf{f}_v \\ \mathbf{f}_w \\ \mathbf{f}_\theta \end{Bmatrix} = \begin{bmatrix} \mathbf{K}_u & \mathbf{0} & \mathbf{0} & \mathbf{0} \\ \mathbf{0} & \mathbf{K}_v & \mathbf{0} & \mathbf{0} \\ \mathbf{0} & \mathbf{0} & \mathbf{K}_w & \mathbf{0} \\ \mathbf{0} & \mathbf{0} & \mathbf{0} & \mathbf{K}_\theta \end{bmatrix} \begin{Bmatrix} \boldsymbol{u}_s \\ \boldsymbol{v}_s \\ \boldsymbol{w} \\ \boldsymbol{\theta} \end{Bmatrix} \tag{13}$$

It should be mentioned that the lateral displacements ($\boldsymbol{u}_s$, $\boldsymbol{v}_s$) of a beam element are defined with respect to the shear center, while $\boldsymbol{w}$ is the average axial displacement of a given section and that it is not necessarily equal to $\boldsymbol{w}_s$.

[$\mathbf{K}_u$], [$\mathbf{K}_v$], and [$\mathbf{K}_w$] are given by the following equations respectively:

$$\begin{Bmatrix} V_{xL} \\ V_{xR} \\ M_{yL} \\ M_{yR} \end{Bmatrix} = \begin{bmatrix} \frac{12EI_{xx}}{\ell^3} & -\frac{12EI_{xx}}{\ell^3} & \frac{6EI_{xx}}{\ell^2} & \frac{6EI_{xx}}{\ell^2} \\ -\frac{12EI_{xx}}{\ell^3} & \frac{12EI_{xx}}{\ell^3} & -\frac{6EI_{xx}}{\ell^2} & -\frac{6EI_{xx}}{\ell^2} \\ \frac{6EI_{xx}}{\ell^2} & -\frac{6EI_{xx}}{\ell^2} & \frac{4EI_{xx}}{\ell} & \frac{2EI_{xx}}{\ell} \\ \frac{6EI_{xx}}{\ell^2} & -\frac{6EI_{xx}}{\ell^2} & \frac{2EI_{xx}}{\ell} & \frac{4EI_{xx}}{\ell} \end{bmatrix} \begin{Bmatrix} u_L \\ u_R \\ u'_L \\ u'_R \end{Bmatrix} \quad \text{or} \quad \{\mathbf{f}_u\} = [\mathbf{K}_u]\{\mathbf{u}_s\} \tag{14}$$

$$\begin{Bmatrix} V_{yL} \\ V_{yR} \\ M_{xL} \\ M_{xR} \end{Bmatrix} = \begin{bmatrix} \frac{12EI_{yy}}{\ell^3} & -\frac{12EI_{yy}}{\ell^3} & \frac{6EI_{yy}}{\ell^2} & \frac{6EI_{yy}}{\ell^2} \\ -\frac{12EI_{yy}}{\ell^3} & \frac{12EI_{yy}}{\ell^3} & -\frac{6EI_{yy}}{\ell^2} & -\frac{6EI_{yy}}{\ell^2} \\ \frac{6EI_{yy}}{\ell^2} & -\frac{6EI_{yy}}{\ell^2} & \frac{4EI_{yy}}{\ell} & \frac{2EI_{yy}}{\ell} \\ \frac{6EI_{yy}}{\ell^2} & -\frac{6EI_{yy}}{\ell^2} & \frac{2EI_{yy}}{\ell} & \frac{4EI_{yy}}{\ell} \end{bmatrix} \begin{Bmatrix} v_L \\ v_R \\ v'_L \\ v'_R \end{Bmatrix} \quad \text{or} \quad \{\mathbf{f}_v\} = [\mathbf{K}_v]\{\boldsymbol{v}_s\} \tag{15}$$

$$\begin{Bmatrix} V_{zL} \\ V_{zR} \end{Bmatrix} = \begin{bmatrix} \frac{EA}{\ell} & -\frac{EA}{\ell} \\ -\frac{EA}{\ell} & \frac{EA}{\ell} \end{bmatrix} \begin{Bmatrix} w_L \\ w_R \end{Bmatrix} \quad \text{or} \quad \{\mathbf{f}_w\} = [\mathbf{K}_w]\{\boldsymbol{w}\} \tag{16}$$

Now the general stiffness matrix which is defined with respect to arbitrary nodal points P and Q can be obtained by a standard transformation procedure of stiffness matrices. That is, the transformation matrix [$\mathbf{T}$] is obtained by using eq. (1) as follows:

$$\begin{Bmatrix} u_s \\ v_s \\ w \\ \theta \end{Bmatrix} = \begin{bmatrix} \mathbf{I} & 0 & 0 & \mathbf{t}_{ys} \\ 0 & \mathbf{I} & 0 & \mathbf{t}_{xs} \\ \mathbf{t}_x & \mathbf{t}_y & \mathbf{I} & \mathbf{t}_\omega \\ 0 & 0 & 0 & \mathbf{I} \end{bmatrix} \begin{Bmatrix} u_{pq} \\ v_{pq} \\ w_{pq} \\ \theta_{pq} \end{Bmatrix} \tag{17}$$

where (u_{pq} , v_{pq} , w_{pq}) are the nodal displacements of given points P and Q and [$\mathbf{I}$] is an unit matrix of (4 x 4) or (2 x 2) and rectangular matrices, [$\mathbf{t}_x$], [$\mathbf{t}_y$], [$\mathbf{t}_{xs}$], [$\mathbf{t}_{ys}$] and [$\mathbf{t}_\omega$] are defined by the following equations:

$$[\mathbf{t}_x] = \begin{bmatrix} 0 & 0 & x_p & 0 \\ 0 & 0 & 0 & x_q \end{bmatrix}, \quad [\mathbf{t}_{xs}] = \begin{bmatrix} -x_{ps} & 0 & 0 & 0 \\ 0 & -x_{qs} & 0 & 0 \\ 0 & 0 & -x_{ps} & 0 \\ 0 & 0 & 0 & -x_{qs} \end{bmatrix}$$

$$[\mathbf{t}_y] = \begin{bmatrix} 0 & 0 & y_p & 0 \\ 0 & 0 & 0 & y_q \end{bmatrix}, \quad [\mathbf{t}_{ys}] = \begin{bmatrix} y_{ps} & 0 & 0 & 0 \\ 0 & y_{qs} & 0 & 0 \\ 0 & 0 & y_{ps} & 0 \\ 0 & 0 & 0 & y_{qs} \end{bmatrix} \tag{18}$$

$$[\mathbf{t}_\omega] = \begin{bmatrix} 0 & 0 & -\omega_{np} & 0 \\ 0 & 0 & 0 & -\omega_{nq} \end{bmatrix},$$

Using the transformation matrix [$\mathbf{T}$] and following the standard procedure the general stiffness matrix [K] of a given beam element is obtained as shown in Table I.
In the similar manner, the mass matrix of a beam element whose nodal points are taken at any point on the each end section can be obtained and it is shown in Table II.

2.4 Shear Deformation Analysis of a Slender Structure [6],[7]

The overall structural analysis so far explained is based on the engineering theory of a beam, so that the effect of shear deformation is neglected. Distribution of shearing stresses ($\tau_{xz}^{(s)}$, $\tau_{yz}^{(s)}$), however, is often important in design of thin-walled structures and in this section finite element analysis on the shear deformation of a beam type structure is developed by basing on the well-known St. Venant's Semi-Inverse Method [8],[9].
By adding the correcting displacements ($U_c(x, y, z)$, $V_c(x, y, z)$, $W_c(x, y, z)$) to eq. (1), the true displacements of a given slender structure can be given as follows:

$$\begin{aligned} U(x,y,z) &= u(z) - y\theta(z) + U_c(x,y,z) \\ V(x,y,z) &= v(z) + x\theta(z) + V_c(x,y,z) \\ W(x,y,z) &= w(z) - xu'(z) - yv'(z) + \theta'(z)\omega_n(x,y) + W_c(x,y,z) \end{aligned} \tag{19}$$

Now assuming that displacements of the idealized beam structure ($u(z)$, $v(z)$, $w(z)$, $\theta(z)$) are known, the correcting displacements (U_c , V_c , W_c) should be determined so as to satisfy the following equilibrium equations:

$$\left.\begin{aligned} \frac{\partial \sigma_x^{(c)}}{\partial x} + \frac{\partial \tau_{xy}^{(c)}}{\partial y} + \frac{\partial \tau_{xz}^{(c)}}{\partial z} + X &= 0 \\ \frac{\partial \tau_{yx}^{(c)}}{\partial x} + \frac{\partial \sigma_y^{(c)}}{\partial y} + \frac{\partial \tau_{yz}^{(c)}}{\partial z} + Y &= 0 \end{aligned}\right\} \tag{20}$$

$$\frac{\partial \tau_{zx}^{(c)}}{\partial x} + \frac{\partial \tau_{zy}^{(c)}}{\partial y} + \frac{\partial \sigma_z^{(c)}}{\partial z} + Z + E(w'' - x u''' - y v''' + \theta''' \omega_n) = 0 \quad \Bigg\}$$

where stresses $\sigma_x^{(c)}$, ..., $\tau_{xy}^{(c)}$, ... etc. are correcting stresses due to additional displacements, and (X , Y , Z) are components of body forces.
The associated boundary conditions of side surface are given as follows by assuming no surface tractions:

$$\left.\begin{aligned} \sigma_x^{(c)} \ell + \tau_{xy}^{(c)} m &= 0 \\ \tau_{yx}^{(c)} \ell + \sigma_y^{(c)} m &= 0 \\ \tau_{zx}^{(c)} \ell + \tau_{zy}^{(c)} m &= 0 \end{aligned}\right\} \tag{21}$$

The equations of virtual work corresponding to eqs. (20) and (21) can be given as follows:

$$\begin{aligned} &\iiint (\sigma_x^{(c)} \delta \varepsilon_x^{(c)} + \sigma_y^{(c)} \delta \varepsilon_y^{(c)} + \sigma_z^{(c)} \delta \varepsilon_z^{(c)} + \tau_{xy}^{(c)} \delta \gamma_{xy}^{(c)} + \tau_{yz}^{(c)} \delta \gamma_{yz}^{(c)} + \tau_{zx}^{(c)} \delta \gamma_{zx}^{(c)}) dV \\ &- \iiint [X \delta U_c + Y \delta V_c + \{Z + E(w' - x u'' - y v'' + \theta'' \omega_n)\} \delta W_c] dV = 0 \end{aligned} \tag{22}$$

In the case of a beam with rigid cross section, U_C = V_C = 0 can be easily concluded without loosing generality, and therefore eq. (22) can be simplified as follows:

$$\begin{aligned} &\delta \iiint \frac{1}{2} \left[G \left\{ \left(\frac{\partial W_c}{\partial x} \right)^2 + \left(\frac{\partial W_c}{\partial y} \right)^2 \right\} + E \left(\frac{\partial W_c}{\partial z} \right)^2 \right] dV \\ &- \iiint \{ Z + E(w' - x u'' - y v'' + \theta'' \omega_n) \} \delta W_c \, dV = 0 \end{aligned} \tag{23}$$

This is the general variational equation for existing shear deformation analysis of a beam which is originated by Saint-Venant and extended by Eric Reissner.
Determination of the distribution of these additional stresses ($\sigma_x^{(c)}$, ... $\tau_{xy}^{(c)}$, ...) is not sufficient for complete shear deformation analysis of a beam, and the effect of shear deformation on the deflection of a given beam should be further analysed. More precisely, additional stresses may give influence on the beam deflection ($u(z)$, $v(z)$, $w(z)$, $\theta(z)$) and the modified beam deflection can be determined by the following equation of virtual work:

$$\begin{aligned} &\delta \int_0^\ell \frac{1}{2} (EA w'^2 + E I_{xx} u_s''^2 + E I_{yy} v_s''^2 + E I_\omega^{(s)} \theta''^2 + GK \theta'^2) dz \\ &- \int_0^\ell (q_x \delta u_s + q_y \delta v_s + p \delta w + m_z \delta \theta) dz \\ &- \int_0^\ell (p^{(c)} \delta w' + m_y^{(c)} \delta u_s'' - m_x^{(c)} \delta v_s'' + m_\omega^{(c)} \delta \theta'') dz = 0 \end{aligned} \tag{24}$$

where $p^{(c)}$, $m_x^{(c)}$, $m_y^{(c)}$, $m_\omega^{(c)}$ are defined as follows:

$$\left.\begin{aligned} p^{(c)} &= \iint \sigma_z^{(c)} dx\,dy \quad , \quad & m_x^{(c)} &= \iint \sigma_z^{(c)} y \, dx\,dy \\ m_y^{(c)} &= -\iint \sigma_z^{(c)} x \, dx\,dy \quad , \quad & m_\omega^{(c)} &= \iint \sigma_z^{(c)} \omega_n \, dx\,dy \end{aligned}\right\} \tag{25}$$

The finite element formulation of the present problem will be described in the following. The true displacement vector of discretized structure u can be expressed as sum of the displacement vector u_I of the idealized beam structure and correction displacement vector u_C

$$u = S_I u_I + S_C u_C \tag{26}$$

By following the standard procedure of the finite element method, the overall stiffness equation of a given structure is finally obtained in the following form:

$$\left[\begin{array}{c|c} K_{II} & K_{IC} \\ \hline K_{CI} & K_{CC} \end{array}\right] \left\{\begin{array}{c} u_I \\ \hline u_C \end{array}\right\} = \left\{\begin{array}{c} Q_I \\ \hline Q_C \end{array}\right\} \tag{27}$$

From which the following matrix equations will be obtained:

$$K_{CC} u_C = Q_C - K_{CI} u_I \tag{28}$$

$$(K_{II} - K_{IC} K_{CC}^{-1} K_{CI}) u_I = Q_I - K_{IC} K_{CC}^{-1} Q_C \tag{29}$$

Eq. (28) can be the stiffness equation for determination of additional displacements, from the solution of which shearing stress distribution can be obtained, while eq. (29) gives the refined stiffness equation of the idealized beam structure in which the effect of shear deformation is taken into account.

Therefore, if the body force is distributed such that $Q_C = 0$, the stiffness equation of a given beam structure will be written as follows:

$$\left.\begin{array}{l} K_{eff} u_I = Q_I \\ K_{eff} = K_{II} - K_S \\ K_S = K_{IC} K_{CC}^{-1} K_{CI} \end{array}\right\} \tag{30}$$

Remembering that the original stiffness equation of the beam is given by

$$K_{II} u_I = Q_I \tag{31}$$

it is concluded that K_{eff} is the effective stiffness of the beam structure in which the stiffness reduction K_S due to shear deformation is considered, and the vibration analysis of the beam structure under the effect of shear deformation can be made by solving the following characteristic equation:

$$| K_{eff} - p^2 M | = 0 \tag{32}$$

From the discussion so far mentioned, it can be seen that the more elaborate vibration as well as deflection analysis can be made by using eqs. (30) and (32) respectively. However it should be mentioned here that such rigorous beam analysis may be essentially nonlinear and therefore these equations are only valid for small additional displacements (U_C, V_C, W_C), because assumption of rigid cross section can not be preserved during the deformation owing to existence of (U_C, V_C).

3. APPLICATION OF THE PRESENT METHOD TO VIBRATION AND RESPONSE ANALYSIS OF A FUEL CHARGING MACHINE OF A NUCLEAR REACTOR

The aseismic design on the FUGEN Charge Machine System as shown in Fig. 3 was made by conducting the vibration and response analysis of a model structure based on the method described so far. This system is to be used for advanced thermal reactor which is developed by the Power Reactor and Nuclear Fuel Development Corporation in Japan.

Idealizing this system as a three dimensional beam structure, eigenvalue analysis, timehistroy response analysis as well as response analysis by response spectra have been made. For experimental verification, vibration test was conducted by using a 1/10 scale model structure.

3.1 Seismic Analysis of FUGEN Charge Machine System

(i) Eigenvalue Analysis

The idealized model structure is shown in Fig. 4. In this analysis model, the traversing truck is idealized as four rigid beams. The traversing truck and the travelling truck beams are pin-connected at the nodal points 2, 3, 6, 7. Results of eigenvalue analysis by using vibration analysis code of 3D beams structures are shown in Fig. 5.

(ii) Time History Response Analysis

In this analysis horizontal and rotational acceleration is considered for input acceleration. The vibration equations of the structure having mass matrix [M], damping matrix [C], and stiffness matrix [K] under horizontal and rotational acceleration inputs $\ddot{y}$ are shown below:

$$[M]\{\ddot{u}\} + [C]\{\dot{u}\} + [K]\{u\} = -\ddot{y}[M]\{\alpha_y\} \tag{33}$$

where, $\{\alpha_y\}$ is the vector representing the effect of the input acceleration $\ddot{y}$ on $\{u\}$. Elements of the modal analysis of eq. (33) are shown below:

$$\{u\} = \sum_{i=1}^{n} q_i \{X_i\} \tag{34}$$

where, q_i : the coefficient of the i-th vibration mode for input

$\{X_i\}$: the eigen vector of the i-th mode

Using the orthogonal condition of eigen vectors and eq. (34), and assuming that the damping factor, C_{ij} is negligibly small, eq. (33) is given as follows:

$$\ddot{q}_i + 2\omega_i h_i \dot{q}_i + \omega_i^2 q_i = -\ddot{y}\beta_i \tag{35-a}$$

where

$$\omega_i^2 = \frac{\{X_i\}^T[K]\{X_i\}}{\{X_i\}^T[M]\{X_i\}} \tag{35-b}$$

$$h_i = \frac{\{X_i\}^T[C]\{X_i\}}{2\{X_i\}^T[M]\{X_i\}\,\omega_i} \tag{35-c}$$

β_i : exciting coefficient

Then, the solution at any time t of eq. (35-a) is given in the following form by using Duhamel integration:

$$q_i = -\frac{\beta_i}{\sqrt{1-h_i^2}\,\omega_i}\int_0^t \ddot{y}(\tau)\exp\{-h_i\omega_i(t-\tau)\}\sin\{\sqrt{1-h_i^2}\,\omega_i(t-\tau)\}\,d\tau \tag{35-d}$$

The dispacement at any nodal point is given by using eq. (35) and eq. (33). The results of response calculation for El Centro earthquake (Fig. 6a, 6b) are shown in Figs. 6c, 6d and 6e. Fig. 6c, Fig. 6d and Fig. 6e show the response displacements of the upper and the lower end of the pressure vessel and the connection between the pressure vessel and the traverse truck, respectively. Input conditions of the above case are:

$h_i = 0.01\, h_c$	h_c :	critical damping factor
considered mode orders	:	from the first to the 6th mode and each eigenvalue and eigen vector are shown in Fig. 5
earthquake input nodal point	:	nodal 1, 4, 5, 8, of Fig. 4
earthquake input direction	:	z direction of Fig. 4

(iii) Seismic Response Analysis by Using Response Spectra

The structure shown in Fig. 4 is again used as the calculation model. The results shown in Fig. 5 are used for eigenvalue and eigen vector, and the results mentioned in previous section (ii) are applied for the exciting coefficients. Here, rotational acceleration is not considered in the exciting coefficients. Representing S_{ai} for the i-th order acceleration of response spectra, the equation of the max. i-th response acceleration $\{\ddot{u}_i + \ddot{y}\}_{max}$ can be obtained by modal analysis as follows:

$$\{\ddot{u}_i + \ddot{y}\}_{max} = \{X_i\}\beta_i S_{ai} \tag{36}$$

The i-th response displacement $\{u_i\}_{max}$ due to the acceleration of eq. (36) is given by:

$$\{u_i\}_{max} \doteq [K]^{-1}[M]\{\ddot{u}_i + \ddot{y}\}_{max} \tag{37}$$

Response value $\{u\}_{max}$ calculated from each mode vector is given by root mean square of each mode response value, that is j element value $u_{j\,max}$ of vector $\{u\}_{max}$ is:

$$u_{j\,max} = \sqrt{\sum_{i=1}^{n} (u_{ji})_{max}^2} \tag{38}$$

where, $(u_{ji})_{max}$ is j element value of $\{u_i\}_{max}$ calculated from i-th vector.

Response displacements at the upper end and the lower end of the pressure vessel calculated by response spectra and the max. response displacement calculated by time history analysis are shown in Table III. In the above response spectra calculation, response spectra values S_a adopted for input data are shown in Table IV. As will be seen easily in Table III, the max. response displacements by time history analysis are in good agreement with the response displacements by response spectra.

3.2 Vibration Model Test

(i) Vibration Testing

Vibration test was performed by using about 1/10 scale model shown in Fig. 7. Forced vibration device and measuring device are shown in Figs. 8a and 8b. The test model is supported at the points A, B, C,.......,K and L of Fig. 7 by pin connections. The pressure vessel in the actual structure was simulated by the spindle in the test model in which stiffness as well as mass distribution were proportionally reduced. The testing methods are explained below:

(1) forced vibration method: non-contact type forced vibrator by electro magnet

(2) forced vibration point and direction:

point - at the lower end of the spindle

direction - z direction of Fig. 7

(3) measuring method: eigen frequencies of testing model are detected by two friction

type gauges attached to the upper and the lower ends of the spindle (points M and N of Fig. 7)

(4) measuring items: eigen frequencies

The testing results are indicated in Fig. 9.

(ii) Eigenvalue Analysis of the Test Model Idealized as a Three Dimensional Plate Structure

It should be mentioned here that results of beam vibration analysis mentioned above is only the first achievement of the present research project, because the computer program for vibration analysis of thin-walled structures where the effects of shear deformation is taken into consideration was not completed.

In order to supplement the results of eigenvalue analysis, vibration analysis of the same structure as composed of plate and beam elements was carried out. Plate element used is a rectangular element whose displacement function is proposed by B. E. Greene and others [11]. In the eigenvalue calculation, mass condensation method proposed by J. N. Ramsden and J. R. Stoker [12] is adopted. The results of calculation are indicated in Fig. 9 where results of the beam vibration analysis as well as experimental data are also shown.

The condition of pin connection assumed in vibration analyses of the testing model shown in Fig. 5 can be hardly satisfied in experiment. Nevertheless it can be concluded by considering possible discrepancy between results of experiment and calculations, that vibration analysis of the charge machine system idealized as a thin-walled structure and based on the proposed method may be duly justified.

4. CONCLUSION

Basing on the modern beam theory, finite element method of analysis of thin-walled structures was proposed in this paper.

Important feature of the present method may be summarized as follows:

(a) Finite element analysis on the St. Venant's torsion problem initiated by Prof. L.R. Herrmann is extended to evaluate various torsional constants such as, I_ω , $I_{\omega x}$, $I_{\omega y}$ and location of shear center.

(b) A new stiffness matrix of the beam element for warping-torsion is developed by using 3rd order polynomial.

(c) Finite element method of analysis of a beam with variable cross section is proposed. This method may be in principle the same as the method proposed by Professor J. H. Argyris, but it may be superior in simplicity of theoretical formulation.

(d) Effects of cut-out or transverse stiffnening members on the section properties of given beam structure can be included in the evaluation of the stiffness matrices although such formulation was not described in this paper because of space limitation.

(e) Size of stiffness equation may seldom exceed several hundreds in the present method so that small computing facilities will be sufficient for the overall analysis of structures at initial design stage.

Application of the present finite element method to vibration analysis of the fuel charge machine of nuclear reactors resulted in good agreement with experimental data of the test model of a thin-walled beam structure.

5. ACKNOWLEDGEMENT

The authors would like to express their great thanks to Prof. H. Shibata, University of Tokyo and all the members who were involved in the FUGEN Project especially Mr. M. Akebi at Power Reactor and Nuclear Fuel Development Corporation, Dr. K. Akino at The Japan Atomic Power Co. and Mr. T. Kuroda at The Electric Power Development Co. for their valuable advice and encouragement. The authors also wish to express their hearty thanks to Mr. Takaichi, Mr. M. Fujita and Mr. I. Yukishima at Fuji Electric Co. for their support. They are also indebted to Mr. Y. Fujitani, Mr. S. Shiina and Miss S. Suzuki for their efforts shown in the preparations of this paper.

6. REFERENCES

[1] HERRMANN, L. R., "Elastic Torsional Analysis of Irregular Shapes", ASCE, Engineering Mechanics Division, Vol. 91, No. EM 6, 11-19 (1965).

[2] KAWAI, T. and YOSHIMURA, N., "Finite Element Analysis on the Torsion of a Bar with Uniform Cross Section", Seisan Kenkyu, Vol. 20, No. 5, May, 246-248 (1968).

[3] KAWAI, T. and others, "Finite Element Analysis of Thin-Walled Structures Based on the Modern Engineering Theory of Beams", Proc. of the third Airforce Conference on Matrix Methods in Structural Mechanics held in Wright Patterson Air Force Base, Ohio (1971).

[4] ARGYRIS, J. H. and RADAJ, D., "Steifigkeitsmatrizen dünnwandiger Stäbe und Stabsysteme", Ingenieur-Archiev 40, 198-210 (1971).

[5] TANAKA, N., SAMBONGI S. and KAWAI, T., " A Torsional Strength Analysis on the Container Ship by Means of the Finite Element Procedure and Full-scale Testing", International Shipbuilding Progress, Shipbuilding and Marine Engineering Monthly, Vol. 18, No. 201, May, 198-214 (1971).

[6] PAYER, H. G., " A Study of the Distribution of Shear in Tankers with Longitudinal Bulkheads subject to Bending", Univ. of California College of Engineering Department of Naval Architecture (1967).

[7] PAULLING, J. R., "Application of the Finite Element Method to Ship Structural Analysis", Japan-U.S. Seminar on Matrix Method of Structural Analysis and Design (1969).

[8] KAWAI, T. and FUJITANI, Y., "Shear Deformation Analysis of a Beam Based on the Finite Element Method", Proc. of J.S.S.C. Symposium on Matrix Method of Structural Analysis and Design, 54-61 (1971).

[9] HERRMANN, L. R., "Elastic Shear Analysis of General Prismatic Beam", Proc. of A.S.C.E., 94, EM 4, 965-983 (1968).

[10] KAWAI, T., "Some Applications of the Finite Element Methods to Ship Structural Aanalysis", Preprinted Abstracts of Symposium Papers, National Symposium on Computerized Structural Analysis and Design, George Washington University, Wash. D.C., May, (1972).

[11] GREENE, B. E., "Stiffness Matrix for Bending of a Rectangular Plate Element with Initial Membrane Stresses", SARM-45.

[12] RAMSDEN, J. N. and STOKER, J. R., "Mass Condensation A Semi-Automatic Method for Reducing the Size of Vibration Problems", Int. J. of Num. Meth., Vol. 1, (1969).

Table I General Stiffness Matrix of a Beam Element Defined with Respect to an Arbitary Nordal Points P and Q on the Beam Cross Section $[k_{pq}]$

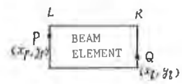

	u_p	u_q	u'_p	u'_q	v_p	v_q	v'_p	v'_q	w_p	w_q	θ_p	θ_q	θ'_p	θ'_q
V_{xL}	$\frac{12EI_{xx}}{\ell^3}$													
V_{xR}	$-\frac{12EI_{xx}}{\ell^3}$	$\frac{12EI_{xx}}{\ell^3}$												
M_{yL}	$\frac{6EI_{xx}}{\ell^2}$	$-\frac{6EI_{xx}}{\ell^2}$	$\frac{4EI_{xx}}{\ell}+\frac{EAy_p^2}{\ell}$											
M_{yR}	$\frac{6EI_{xx}}{\ell^2}$	$-\frac{6EI_{xx}}{\ell^2}$	$\frac{2EI_{xx}}{\ell}-\frac{EAy_py_q}{\ell}$	$\frac{4EI_{xx}}{\ell}+\frac{EAy_q^2}{\ell}$										
V_{yL}	0	0	0	0	$\frac{12EI_{yy}}{\ell^3}$									
V_{yR}	0	0	0	0	$-\frac{12EI_{yy}}{\ell^3}$	$\frac{12EI_{yy}}{\ell^3}$								
M_{xL}	0	0	$\frac{EAx_py_p}{\ell}$	$-\frac{EAx_qy_p}{\ell}$	$\frac{6EI_{yy}}{\ell^2}$	$-\frac{6EI_{yy}}{\ell^2}$	$\frac{4EI_{yy}}{\ell}+\frac{EAx_p^2}{\ell}$							
M_{xR}	0	0	$-\frac{EAx_py_q}{\ell}$	$\frac{EAx_qy_q}{\ell}$	$\frac{6EI_{yy}}{\ell^2}$	$-\frac{6EI_{yy}}{\ell^2}$	$\frac{2EI_{yy}}{\ell}-\frac{EAx_px_q}{\ell}$	$\frac{4EI_{yy}}{\ell}+\frac{EAx_q^2}{\ell}$						
V_{zL}	0	0	$\frac{EAx_p}{\ell}$	$-\frac{EAx_q}{\ell}$	0	0	$\frac{EAy_p}{\ell}$	$-\frac{EAy_q}{\ell}$	$\frac{EA}{\ell}$					
V_{zR}	0	0	$-\frac{EAx_p}{\ell}$	$\frac{EAx_q}{\ell}$	0	0	$-\frac{EAy_p}{\ell}$	$\frac{EAy_q}{\ell}$	$-\frac{EA}{\ell}$	$\frac{EA}{\ell}$				
M_{zL}	$\frac{12EI_{xp}}{\ell^3}$	$-\frac{12EI_{xp}}{\ell^3}$	$\frac{6EI_{xp}}{\ell^2}$	$\frac{6EI_{xp}}{\ell^2}$	$\frac{12EI_{yp}}{\ell^3}$	$-\frac{12EI_{yp}}{\ell^3}$	$\frac{6EI_{yp}}{\ell^2}$	$\frac{6EI_{yp}}{\ell^2}$	0	0	$\frac{12EI_{\omega p}}{\ell^3}+\frac{6GK}{5\ell}$			
M_{zR}	$-\frac{12EI_{xq}}{\ell^3}$	$\frac{12EI_{xq}}{\ell^3}$	$-\frac{6EI_{xq}}{\ell^2}$	$-\frac{6EI_{xq}}{\ell^2}$	$-\frac{12EI_{yq}}{\ell^3}$	$\frac{12EI_{yq}}{\ell^3}$	$-\frac{6EI_{yq}}{\ell^2}$	$-\frac{6EI_{yq}}{\ell^2}$	0	0	$-\frac{12EI_{\omega pq}}{\ell^3}-\frac{6GK}{5\ell}$	$\frac{12EI_{\omega q}}{\ell^3}+\frac{6GK}{5\ell}$		
T_L	$\frac{6EI_{xp}}{\ell^2}$	$-\frac{6EI_{xp}}{\ell^2}$	$\frac{4EI_{xp}}{\ell}-\frac{EAx_p\omega_{np}}{\ell}$	$\frac{2EI_{xp}}{\ell}+\frac{EAx_q\omega_{np}}{\ell}$	$\frac{6EI_{yp}}{\ell^2}$	$-\frac{6EI_{yp}}{\ell^2}$	$\frac{4EI_{yp}}{\ell}-\frac{EAy_p\omega_{np}}{\ell}$	$\frac{2EI_{yp}}{\ell}+\frac{EAy_q\omega_{np}}{\ell}$	$-\frac{EA\omega_{np}}{\ell}$	$\frac{EA\omega_{np}}{\ell}$	$\frac{6EI_{\omega p}}{\ell^2}+\frac{GK}{10}$	$-\frac{6EI_{\omega pq}}{\ell^2}-\frac{GK}{10}$	$\frac{4EI_{\omega p}}{\ell}+\frac{2\ell GK}{15}+\frac{EA\omega_{np}^2}{\ell}$	
T_R	$\frac{6EI_{xq}}{\ell^2}$	$-\frac{6EI_{xq}}{\ell^2}$	$\frac{2EI_{xq}}{\ell}+\frac{EAx_p\omega_{nq}}{\ell}$	$\frac{4EI_{xq}}{\ell}-\frac{EAx_q\omega_{nq}}{\ell}$	$\frac{6EI_{yq}}{\ell^2}$	$-\frac{6EI_{yq}}{\ell^2}$	$\frac{2EI_{yq}}{\ell}+\frac{EAy_p\omega_{nq}}{\ell}$	$\frac{4EI_{yq}}{\ell}-\frac{EAy_q\omega_{nq}}{\ell}$	$\frac{EA\omega_{nq}}{\ell}$	$-\frac{EA\omega_{nq}}{\ell}$	$\frac{6EI_{\omega pq}}{\ell^2}+\frac{GK}{10}$	$-\frac{6EI_{\omega q}}{\ell^2}-\frac{GK}{10}$	$\frac{2EI_{\omega pq}}{\ell}-\frac{\ell GK}{30}-\frac{EA\omega_{np}\omega_{nq}}{\ell}$	$\frac{4EI_{\omega q}}{\ell}+\frac{2\ell GK}{15}+\frac{EA\omega_{nq}^2}{\ell}$

$I_{xp} = y_{ps}I_{xx} = y_pI_{xx} - I_{\omega x}$, $I_{xq} = y_{qs}I_{xx} = y_qI_{xx} - I_{\omega x}$

$I_{yp} = x_{ps}I_{yy} = x_pI_{yy} + I_{\omega y}$, $I_{yq} = x_{qs}I_{yy} = x_qI_{yy} + I_{\omega y}$

$I_{\omega p} = I_\omega^{(s)} + y_{ps}^2I_{xx} + x_{ps}^2I_{yy} = I_\omega + y_p^2I_{xx} + x_p^2I_{yy} - 2y_pI_{\omega x} + 2x_pI_{\omega y}$

$I_{\omega q} = I_\omega^{(s)} + y_{qs}^2I_{xx} + x_{qs}^2I_{yy} = I_\omega + y_q^2I_{xx} + x_q^2I_{yy} - 2y_qI_{\omega x} + 2x_qI_{\omega y}$

$I_{\omega pq} = I_\omega^{(s)} + y_{ps}y_{qs}I_{xx} + x_{ps}x_{qs}I_{yy}$

$= I_\omega + y_py_qI_{xx} + x_px_qI_{yy} - (y_p+y_q)I_{\omega x} + (x_p+x_q)I_{\omega y}$

$\omega_{np} = \omega_n(x_p, y_p) - x_py_s + x_sy_p$

$\omega_{nq} = \omega_n(x_q, y_q) - x_qy_s + x_sy_q$

SYM.

Table II General Mass Matrix of a Beam Element Defined with Respect to an Arbitary Nordal Points P and Q on the Beam Cross Section $\frac{\gamma}{g} \times [m_{pq}]$

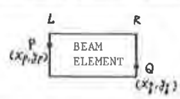

	$\ddot{u}_p$	$\ddot{u}_q$	$\ddot{u}'_p$	$\ddot{u}'_q$	$\ddot{v}_p$	$\ddot{v}_q$	$\ddot{v}'_p$	$\ddot{v}'_q$	$\ddot{w}_p$	$\ddot{w}_q$	$\ddot{\theta}_p$	$\ddot{\theta}_q$	$\ddot{\theta}'_p$	$\ddot{\theta}'_q$
V_{xL}	$\frac{13\ell A}{35}+\frac{6I_{xx}}{5\ell}$													
V_{xR}	$\frac{9\ell A}{70}-\frac{6I_{xx}}{5\ell}$	$\frac{13\ell A}{35}+\frac{6I_{xx}}{5\ell}$												
M_{yL}	$\frac{11\ell^2A}{210}+\frac{I_{xx}}{10}$	$\frac{13\ell^2A}{420}-\frac{I_{xx}}{10}$	$\frac{\ell^3A}{105}+\frac{2\ell I_{xx}}{15}+\frac{\ell Ax_p^2}{3}$											
M_{yR}	$-\frac{13\ell^2A}{420}+\frac{I_{xx}}{10}$	$-\frac{11\ell^2A}{210}-\frac{I_{xx}}{10}$	$-\frac{\ell^3A}{140}-\frac{\ell I_{xx}}{30}+\frac{\ell Ax_px_q}{6}$	$\frac{\ell^3A}{105}+\frac{2\ell I_{xx}}{15}+\frac{\ell Ax_q^2}{3}$										
V_{yL}	0	0	0	0	$\frac{13\ell A}{35}+\frac{6I_{yy}}{5\ell}$									
V_{yR}	0	0	0	0	$\frac{9\ell A}{70}-\frac{6I_{yy}}{5\ell}$	$\frac{13\ell A}{35}+\frac{6I_{yy}}{5\ell}$								
M_{xL}	0	0	$\frac{\ell Ax_py_p}{3}$	$\frac{\ell Ax_qy_p}{6}$	$\frac{11\ell^2A}{210}+\frac{I_{yy}}{10}$	$\frac{13\ell^2A}{420}-\frac{I_{yy}}{10}$	$\frac{\ell^3A}{105}+\frac{2\ell I_{yy}}{15}+\frac{\ell Ay_p^2}{3}$							
M_{xR}	0	0	$\frac{\ell Ax_py_q}{6}$	$\frac{\ell Ax_qy_q}{3}$	$-\frac{13\ell^2A}{420}+\frac{I_{yy}}{10}$	$-\frac{11\ell^2A}{210}-\frac{I_{yy}}{10}$	$-\frac{\ell^3A}{140}-\frac{\ell I_{yy}}{30}+\frac{\ell Ay_py_q}{6}$	$\frac{\ell^3A}{105}+\frac{2\ell I_{yy}}{15}+\frac{\ell Ay_q^2}{3}$						
V_{zL}	0	0	$\frac{\ell Ax_p}{3}$	$\frac{\ell Ax_q}{6}$	0	0	$\frac{\ell Ay_p}{3}$	$\frac{\ell Ay_q}{6}$	$\frac{\ell A}{3}$					
V_{zR}	0	0	$\frac{\ell Ax_p}{6}$	$\frac{\ell Ax_q}{3}$	0	0	$\frac{\ell Ay_p}{6}$	$\frac{\ell Ay_q}{3}$	$\frac{\ell A}{6}$	$\frac{\ell A}{3}$				
M_{zL}	$\frac{13\ell Ay_p}{35}+\frac{6I_{xp}}{5\ell}$	$\frac{9\ell Ay_p}{70}-\frac{6I_{xp}}{5\ell}$	$\frac{11\ell^2Ay_p}{210}+\frac{I_{xp}}{10}$	$-\frac{13\ell^2Ay_p}{420}+\frac{I_{xp}}{10}$	$-\frac{13\ell Ax_p}{35}+\frac{6I_{yp}}{5\ell}$	$-\frac{9\ell Ax_p}{70}-\frac{6I_{yp}}{5\ell}$	$-\frac{11\ell^2Ax_p}{210}+\frac{I_{yp}}{10}$	$\frac{13\ell^2Ax_p}{420}+\frac{I_{yp}}{10}$	0	0	$\frac{13\ell I_{op}}{35}+\frac{6I_{\omega p}}{5\ell}$			
M_{zR}	$\frac{9\ell Ay_q}{70}-\frac{6I_{xq}}{5\ell}$	$\frac{13\ell Ay_q}{35}+\frac{6I_{xq}}{5\ell}$	$\frac{13\ell^2Ay_q}{420}-\frac{I_{xq}}{10}$	$-\frac{11\ell^2Ay_q}{210}-\frac{I_{xq}}{10}$	$-\frac{9\ell Ax_q}{70}-\frac{6I_{yq}}{5\ell}$	$-\frac{13\ell Ax_q}{35}+\frac{6I_{yq}}{5\ell}$	$-\frac{13\ell^2Ax_q}{420}-\frac{I_{yq}}{10}$	$\frac{11\ell^2Ax_q}{210}-\frac{I_{yq}}{10}$	0	0	$\frac{9\ell I_{opq}}{70}-\frac{6I_{\omega pq}}{5\ell}$	$\frac{13\ell I_{oq}}{35}+\frac{6I_{\omega q}}{5\ell}$		
T_L	$\frac{11\ell^2Ay_p}{210}+\frac{I_{xp}}{10}$	$\frac{13\ell^2Ay_p}{420}-\frac{I_{xp}}{10}$	$\frac{\ell^3Ay_p}{105}+\frac{2\ell I_{xp}}{15}-\frac{\ell Ax_p\omega_{np}}{3}$	$-\frac{\ell^3Ay_p}{140}-\frac{\ell I_{xp}}{30}-\frac{\ell Ax_q\omega_{np}}{6}$	$-\frac{11\ell^2Ax_p}{210}+\frac{I_{yp}}{10}$	$-\frac{13\ell^2Ax_p}{420}-\frac{I_{yp}}{10}$	$-\frac{\ell^3Ax_p}{105}+\frac{2\ell I_{yp}}{15}-\frac{\ell Ay_p\omega_{np}}{3}$	$\frac{\ell^3Ax_p}{140}-\frac{\ell I_{yp}}{30}-\frac{\ell Ay_q\omega_{np}}{6}$	$-\frac{\ell A\omega_{np}}{3}$	$-\frac{\ell A\omega_{np}}{6}$	$\frac{11\ell^2I_{op}}{210}+\frac{I_{\omega p}}{10}$	$\frac{13\ell^2I_{opq}}{420}-\frac{I_{\omega pq}}{10}$	$\frac{\ell^3I_{op}}{105}+\frac{2\ell I_{\omega p}}{15}+\frac{\ell A\omega_{np}^2}{3}$	
T_R	$-\frac{13\ell^2Ay_q}{420}+\frac{I_{xq}}{10}$	$-\frac{11\ell^2Ay_q}{210}-\frac{I_{xq}}{10}$	$-\frac{\ell^3Ay_q}{140}-\frac{\ell I_{xq}}{30}-\frac{\ell Ax_p\omega_{nq}}{6}$	$\frac{\ell^3Ay_q}{105}+\frac{2\ell I_{xq}}{15}-\frac{\ell Ax_q\omega_{nq}}{3}$	$\frac{13\ell^2Ax_q}{420}+\frac{I_{yq}}{10}$	$\frac{11\ell^2Ax_q}{210}-\frac{I_{yq}}{10}$	$\frac{\ell^3Ax_q}{140}-\frac{\ell I_{yq}}{30}-\frac{\ell Ay_p\omega_{nq}}{6}$	$-\frac{\ell^3Ax_q}{105}+\frac{2\ell I_{yq}}{15}-\frac{\ell Ay_q\omega_{nq}}{3}$	$-\frac{\ell A\omega_{nq}}{6}$	$-\frac{\ell A\omega_{nq}}{3}$	$-\frac{13\ell^2I_{opq}}{420}+\frac{I_{\omega pq}}{10}$	$-\frac{11\ell^2I_{oq}}{210}-\frac{I_{\omega q}}{10}$	$-\frac{\ell^3I_{opq}}{140}-\frac{\ell I_{\omega pq}}{30}+\frac{\ell A\omega_{np}\omega_{nq}}{6}$	$\frac{\ell^3I_{oq}}{105}+\frac{2\ell I_{\omega q}}{15}+\frac{\ell A\omega_{nq}^2}{3}$

$I_{xp} = y_{ps}I_{xx} = y_pI_{xx} - I_{\omega x}$, $I_{xq} = y_{qs}I_{xx} = y_qI_{xx} - I_{\omega x}$

$I_{yp} = x_{ps}I_{yy} = x_pI_{yy} + I_{\omega y}$, $I_{yq} = x_{qs}I_{yy} = x_qI_{yy} + I_{\omega y}$

$I_{\omega p} = I_\omega^{(s)} + y_{ps}^2I_{xx} + x_{ps}^2I_{yy} = I_\omega + y_p^2I_{xx} + x_p^2I_{yy} - 2y_pI_{\omega x} + 2x_pI_{\omega y}$

$I_{\omega q} = I_\omega^{(s)} + y_{qs}^2I_{xx} + x_{qs}^2I_{yy} = I_\omega + y_q^2I_{xx} + x_q^2I_{yy} - 2y_qI_{\omega x} + 2x_qI_{\omega y}$

$I_{\omega pq} = I_\omega^{(s)} + y_{ps}y_{qs}I_{xx} + x_{ps}x_{qs}I_{yy}$

$= I_\omega + y_py_qI_{xx} + x_px_qI_{yy} - (y_p+y_q)I_{\omega x} + (x_p+x_q)I_{\omega y}$

$\omega_{np} = \omega_n(x_p, y_p) - x_py_s + x_sy_p$

$\omega_{nq} = \omega_n(x_q, y_q) - x_qy_s + x_sy_q$

$I_{op} = I_o + A(x_p^2 + y_p^2)$, $I_{oq} = I_o + A(x_q^2 + y_q^2)$

$I_{opq} = I_o + A(x_px_q + y_py_q)$, $I_o = I_{xx} + I_{yy}$

SIM.

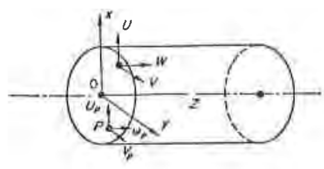

Fig. 1. Coordinate and Notations Employed

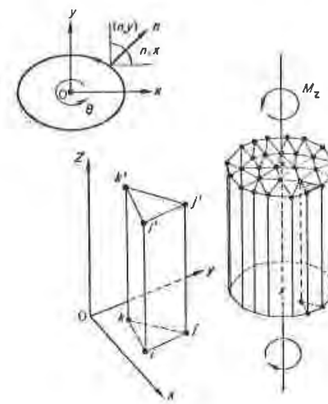

Fig. 2. FEM Analysis of St. Venant's Torsion Problem by a Triangular Prism Element

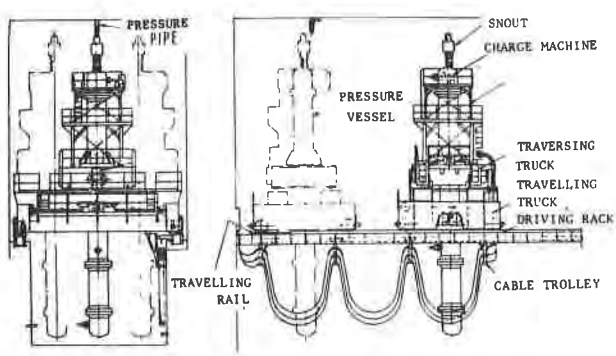

Fig. 3. Charge Machine System

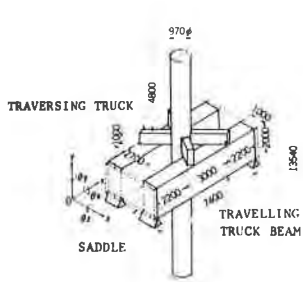

Fig. 4a. Calculation Model for "FUGEN" Charge Machine System

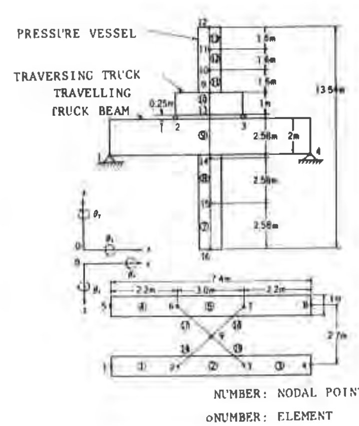

Fig. 4b. Nodal Point Number

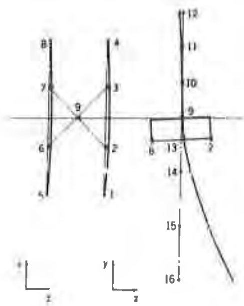

Fig. 5a. The First Mode (PERIOD 0.104 SEC.)

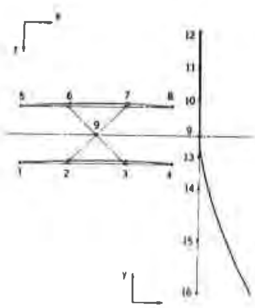

Fig. 5b. The Second Mode (PERIOD 0.104 SEC.)

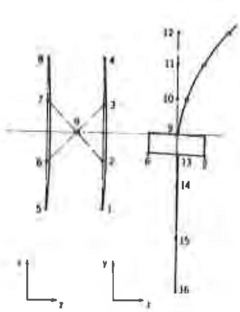

Fig. 5c. The Third Mode (PERIOD 0.0463 SEC.)

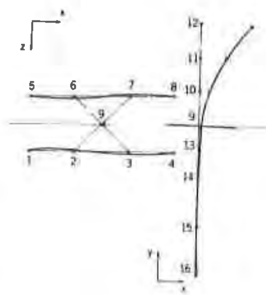

Fig. 5d. The Fourth Mode (PERIOD 0.0447 SEC.)

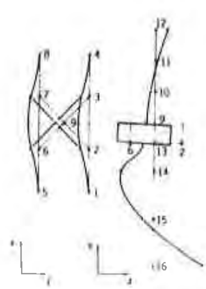

Fig. 5e. The Fifth Mode (PERIOD 0.0186 SEC.)

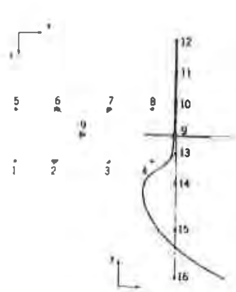

Fig. 5f. The Sixth Mode (PERIOD 0.0171 SEC.)

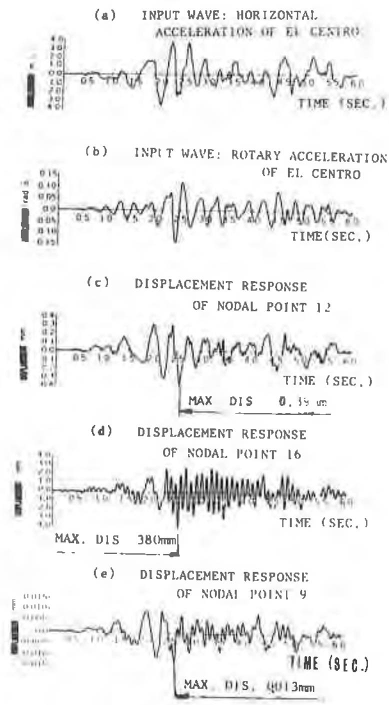

Fig. 6. Response Wave of Charge Machine System due to El Centro Earthquake

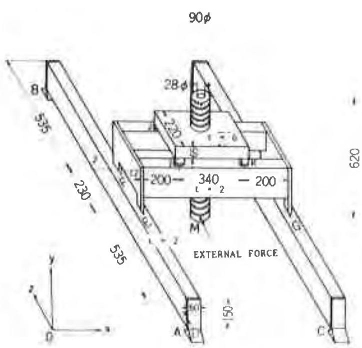

Fig. 7. Dimensions of Test Model (Unit: mm)

Fig. 8a. Vibration Test of Charge Machine Model

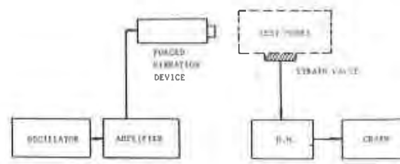

Fig. 8b. Testing Chart

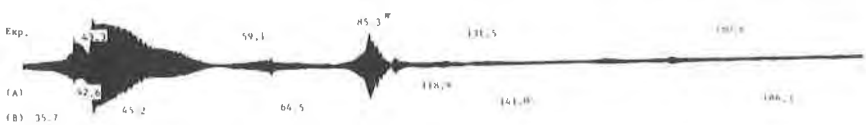

Exp. ; EXPERIMENTAL VALUE

(A) ; BEAM STRUCTURE ANALYSIS (B) ; THIN WALLED STRUCTURE ANALYSIS

Fig. 9. Experimental and Calculation Values

Table III Response Displacements due to El Centro (mm)

	MAX. DISPLACEMENT BY TIME HISTORY ANALYSIS	DISPLACEMENT BY RESPONSE SPECTRA ANALYSIS
TOP OF PRESSURE VESSEL	0.39	0.55
BOTTOM OF PRESSURE VESSEL	3.80	4.01

Table IV Values of Response Spectrum of El Centro

ODER	PERIOD (SEC.)	Sa (g)
1	0.104	0.96
2	0.104	0.96
3	0.0463	0.58
4	0.0447	0.58
5	0.0186	0.58
6	0.0171	0.58